frontiers | Frontiers in Physics

TYPE Review
PUBLISHED 15 September 2023
DOI 10.3389/fphy.2023.1242668

OPEN ACCESS

EDITED BY
Valdir Guimaraes,
University of São Paulo, Brazil

REVIEWED BY
Zilong Chang,
Indiana University, United States
Magda Cicerchia,
University of Padua, Italy

*CORRESPONDENCE
K. L. Jones,
kgrzywac@utk.edu

RECEIVED 19 June 2023
ACCEPTED 28 August 2023
PUBLISHED 15 September 2023

CITATION
Jones KL, Kovoor J and Kanungo R (2023), Status of experimental knowledge on the unbound nucleus ^{13}Be. *Front. Phys.* 11:1242668. doi: 10.3389/fphy.2023.1242668

Status of experimental knowledge on the unbound nucleus ^{13}Be

K. L. Jones[1]*, J. Kovoor[1] and R. Kanungo[2,3]

[1]Department of Physics and Astronomy, University of Tennessee, Knoxville, TN, United States, [2]Astronomy and Physics Department, Saint Mary's University, Halifax, NS, Canada, [3]TRIUMF, Vancouver, BC, Canada

The structure of the unbound nucleus ^{13}Be is important for understanding the Borromean, two-neutron halo nucleus ^{14}Be. The experimental studies conducted over the last four decades are reviewed in the context of the beryllium chain of isotopes and some significant theoretical studies. The focus of this paper is the comparison of new data from a ^{12}Be(d,p) reaction in inverse kinematics, which was analyzed using Geant4 simulations and a Bayesian fitting procedure, with previous measurements. Two possible scenarios to explain the strength below 1 MeV above the neutron separation energy were proposed in that study: a single p-wave resonance or a mixture of an s-wave virtual state with a weaker p- or d-wave resonance. Comparisons of recent invariant mass and the (d,p) experiments show good agreement between the transfer measurement and the two most recent high-energy nucleon removal measurements.

KEYWORDS

direct reactions, clustering, beryllium, ^{13}Be, ^{12}Be

1 Introduction

With just four protons, the particle-bound members of the beryllium chain of isotopes stretch from ^{7}Be ($N/Z = 0.75$) on the proton-rich side of stability to ^{14}Be ($N/Z = 2.5$), the two-neutron halo on the neutron-rich side. Adding a single neutron to ^{7}Be results in the ^{8}Be system of two α particles which is unbound by only 92 keV. Adding a second neutron produces ^{9}Be, the only beryllium isotope that is stable against β decay. This stability is a product of two phenomena that occur across the beryllium chain of isotopes, molecular structures [1]; [2]; [3], and core excitation [4]. The molecular structure is closely connected to the Borromean nature of ^{9}Be; the three-body system of $\alpha - \alpha - n$ is bound despite the two-body subsystems, $\alpha - n$ and $\alpha - \alpha$, being unbound. The delocalized neutron in ^{9}Be can be viewed as being exchanged between α particles [5]. Analogous to atomic molecules, the neutron in the ground state of ^{9}Be is well understood as being in a π-type orbital, whereas the first excited state may be better described with a neutron in the σ-type orbital. These molecular orbits are intimately related to the prolate nature of the two-α cluster structure [6].

The cluster structure appears to weaken in ^{10}Be, as evidenced by the reduced size of its charge radius [7]; [8]. The two-α plus two-neutron structure is more apparent in excited states closer to the α and neutron separation energies, such as the isomeric second 0^+ state at E_x = 6.179 MeV, which has a small γ branch to the more compact first 2^+ state [5].

Adding another neutron makes the archetypal one-neutron halo nucleus ^{11}Be. A 16% core-excited component in the ground state of ^{11}Be was required to reproduce the results from the ^{11}Be(p,d)^{10}Be reaction [9]. This is less than that of ^{9}Be, where the core-excited component was calculated as approximately half of the ground-state wave function [4]. Additionally, dynamical core excitation needs to be included in the calculations of both transfer [10] and breakup [11] reactions.

TABLE 1 Energy (and J^{π} assignments) of low-lying states in ^{13}Be according to a selection of theoretical studies.

Author (year)	Energy above the neutron threshold (MeV)	
	Ground state	Strength 2
Poppelier et al. [20]	1.16 $(\frac{1}{2}^{-})^{a}$	2.44 $(\frac{5}{2}^{-})$
Lenske Ostrowski et al. [30]	0.9 $(\frac{1}{2}^{+})$	2.3 $(\frac{3}{2}^{-})$ and 2.45 $(\frac{5}{2}^{+})$
Descouvemont [23] v2	−0.009 $(\frac{1}{2}^{+})$	2.02 $(\frac{5}{2}^{+})$
Descouvemont [23] v4	−0.038 $(\frac{1}{2}^{+})$	2.05 $(\frac{5}{2}^{+})$
Fortune [21]	0.86 $(\frac{1}{2}^{+})$	2.11 $(\frac{5}{2}^{+})$

[a]Poppelier also calculates a $(\frac{5}{2}^{+})$ state at 1.21 MeV.
Strength 2 refers to any virtual states or resonances approximately 2 MeV above the neutron threshold.

The parity inversion in ^{11}Be, where the $1/2^{+}$ ground state decreases 320 keV below the only other bound state with $J^{\pi} = 1/2^{-}$, along with larger collectivity in ^{10}Be, led to the questioning about the robustness of the $N = 8$ shell closure at ^{12}Be. Using a three-body model with core excitation, Nunes et al. were able to show an increased sphericity in the core ^{10}Be within ^{12}Be compared to that observed in ^{11}Be [12]. This in turn led to greater mixing between *p*- and *sd*-shell valence neutron states and a melting of the $N = 8$ shell closure. The coupling of a *d*-wave neutron with the excited 2^{+} ^{10}Be core severely restricts the formation of a halo in ^{12}Be [13]. Notably, ^{12}Be is not Borromean, as the n-^{10}Be system is bound but is still well described by three-body models.

The $N = 10$ isotope ^{14}Be presents the heaviest particle-stable beryllium isotope. The naive shell model would predict a $d_{5/2}$-dominated ground-state wave function for ^{14}Be. However, with the level inversion seen in the other neutron-rich beryllium isotopes, some low-lying $s_{1/2}$ strength is expected. With two neutrons in the halo and with significant $\ell > 0$ components of the wave function, the halo of ^{14}Be is much more contained than that of ^{11}Be, despite being closer to the drip line. It would seem natural to study ^{14}Be in a three-body model, with ^{12}Be as the core and two valence neutrons [14]; [15]. Thompson and Zhukov found that adding an *s*-wave virtual state below the well-known $\frac{5}{2}^{+}$ state bound ^{13}Be, in contradiction to its non-observance in fragmentation reactions. Reducing the energy, i.e., increasing the scattering length, of the virtual state resulted in the binding energy of ^{14}Be being too low. The three-body approach of Descouvemont found that only 66% of the ground-state wave function of ^{14}Be could be described as ^{12}Be $+n + n$ [14]. Labiche et al. [16], using the model of Vinh Mau and Pacheco [17], found that assuming a $\frac{1}{2}^{-}$ ground state for ^{13}Be, consistent with the melting of the $N = 8$ shell closure observed in ^{11}Be and ^{10}Li, could reproduce the measured properties of ^{14}Be.

Beyond the neutron drip line, ^{15}Be has been observed to decay to ^{12}Be through unbound states in ^{14}Be [18]. The last isotope to be observed is ^{16}Be, which is bound with respect to one neutron emission, but unbound to the emission of two neutrons [19]. The two neutrons from the decay were observed in a small emission angle.

2 The unbound nucleus ^{13}Be

Theoretical studies of ^{13}Be have used the shell model [20] or a potential model [21], the Nilsson model [22], microscopic cluster models [23], antisymmetrized molecular dynamics [24], and relativistic mean-field theory [25]. As shown in Table 1, with the exception of the earliest work, the calculations agree on the existence of a $5/2^{+}$ resonance between 2 and 2.5 MeV above the neutron threshold. However, the location of the ground state relative to the neutron threshold is disputed, as is the parity of the ground state. There have also been reaction theory studies of, and comparing to, experimental data, for example, the work of Bonaccorso [26] and references therein. Casal et al. [27] used a transfer to the continuum model including deformation in the ^{12}Be + n potential, following the prescription in Thompson et al. [28], to interpret the data obtained from Corsi et al. [29]. This work indicates a *p*-wave resonance at between 0.4 and 0.5 MeV above the threshold.

There have been many experiments on ^{13}Be since the first discovery of a resonance [31] at 1.8 MeV above the neutron threshold. Some of the experimental results from the last four decades are shown in Table 2. The reactions used to probe the structure of halo nuclei can be broadly divided into missing mass and invariant mass techniques. Transfer reactions, where excitation energies are found from the reaction Q-values, fall into the missing mass category. Knockout, breakup, and Coulomb dissociation, where the final state is reconstructed from two or more fragments, represent invariant mass techniques. In the case of ^{13}Be, the fragments are ^{12}Be and a neutron. The early measurements, e.g., [31]; [30]; [32]; and [33], mostly populated ^{13}Be through multinucleon transfer reactions. An exception is the ^{12}Be(d,p) experiment performed in [34] at RIKEN. At a beam energy of 55 AMeV, the conditions are not well matched to observe low ℓ transfer, and the carbon in the target largely masked any structure below 2 MeV. Indeed, none of the experiments before the fragmentation experiment at the National Superconducting Cyclotron Laboratory [35] revealed any structure below the $\frac{5}{2}^{+}$ resonance at 2 MeV.

Most of the more recent experiments used invariant mass techniques at energies between 40 and 400 AMeV. Of these, all except one employed nucleon removal, either a neutron from ^{14}Be [37]; [38]; [39]; and [29] or a proton from ^{14}B [36]; [40]; and [42]. In [41], a nucleon exchange reaction was used to populate unbound states in ^{13}Be from a ^{13}B beam. Spectra from invariant mass methods contain information relating to the initial state of the target (the beam in an inverse kinematics reaction) and reflect final state interactions between outgoing fragments. There can also be complications relating to the reaction mechanism, which can be diffractive or absorptive.

TABLE 2 Previous studies of the low-lying structure of ^{13}Be, up to approximately 2.5 MeV above the neutron threshold.

Author (year)	Reaction	Energy above the threshold (MeV) or (a_s) and J^π		
		Ground state (strength 1a)	Strength 1b	Strength 2
Aleksandrov et al. [31]	^{14}C + ^{7}Li	—	—	1.8
Ostrowski et al. [30]	^{13}C + ^{14}C		—	2.01 ($\frac{5}{2}^+$ or $\frac{1}{2}^-$)
Korsheninnikov et al. [34]	^{12}Be + d	—	—	2.0
von Oertzen et al. [32]	^{13}C + ^{14}C	—	—	2.01 ($\frac{5}{2}^+$)
Belozyorov et al. [33]	^{14}C + ^{11}B	—	0.80	2.02
Thoennessen et al. [35]	^{9}Be + ^{18}O	0.20 ($\frac{1}{2}^+$)	0.80 ($\frac{1}{2}$)	2.02 ($\frac{5}{2}^+$)
Lecouey [36]	^{14}B + C	—	0.7 ($\frac{1}{2}^+$)	2.4 ($\frac{5}{2}^+$)
Simon et al. [37]	^{14}Be + C	(−3.2 fm^{-1}) ($\frac{1}{2}^+$)	—	2.00 ($\frac{5}{2}^+$)
Kondo et al. [38]	^{14}Be + p	(−3.4 fm^{-1}) ($\frac{1}{2}^+$)	0.51 ($\frac{1}{2}^-$)	2.39 ($\frac{5}{2}^+$)
Aksyutina et al. [39]	^{14}Be + p	0.46 ($\frac{1}{2}^+$)	—	1.95 ($\frac{5}{2}^+$)
Randisi et al. [40]	^{14,15}B + ^{nat}C	0.40 ($\frac{1}{2}^+$)	0.85 ($\frac{5}{2}^+$)	2.35 ($\frac{5}{2}^+$)
Marks et al. [41]	^{13}B + ^{9}Be	—	0.73 ($\frac{1}{2}^+$)	2.56 ($\frac{5}{2}^+$)
Ribeiro et al. [42]	^{14}B + CH_2	0.44 ($\frac{1}{2}^-$)	0.86 ($\frac{1}{2}^+$)	2.11 ($\frac{5}{2}^+$)
Corsi et al. [29]	^{14}Be + p	(−9.2 fm^{-1}) ($\frac{1}{2}^+$)	0.48 ($\frac{1}{2}^-$)	2.30 ($\frac{5}{2}^+$)
Kovoor et al. [43] single	^{12}Be + ^{solid}D	0.55 ($\frac{1}{2}^-$)	—	2.22 ($\frac{5}{2}^+$)
Kovoor et al. [43] mix	^{12}Be + ^{solid}D	0 − 1 MeV ($\frac{1}{2}^+$) and ($\frac{1}{2}^-$)[a]		2.22 ($\frac{5}{2}^+$)

[a]Order undetermined (see text).
Strength is defined as a single resonance, or a virtual state, or a mixture of resonances, or a virtual state and a resonance. All experiments found some strength below 0.5 MeV above the neutron threshold, and that is labeled as the ground state in this table. Strength 1b is approximately 0.5–0.9 MeV above the neutron threshold. Strength 2 is the well-known *d*-wave resonance at approximately 2 MeV above the neutron threshold, where the literature reports scattering length instead of energy which is quoted in parentheses.

3 Recent transfer reaction measurement

The most recent experiment, [44]; [43], used a ^{12}Be beam from ISAC-II and the solid deuterium target and detector system IRIS [45] to perform a one-neutron transfer reaction. The advantages of using the (d,p) reaction at low energy (E_{beam} = 9.5 AMeV) are that the energy and angular momentum-matching conditions are ideal for populating low-ℓ, near-threshold states. The non-Gaussian experimental response caused by increasingly poor resolution for lower-energy protons exiting the solid deuterium target necessitated an analysis technique that included both simulation and Bayesian fitting methods, as demonstrated in [46]. The initial analysis included the $\frac{5}{2}^+$ resonance at approximately 2 MeV and a single *s*-, *p*-, or *d*-wave virtual state or resonance closer to the threshold, referenced as "single" in Table 2. Additionally, mixes of two out of *s*-, *p*-, and *d*-wave strengths were included to allow for two resonances or a resonance and a virtual state below the 2 MeV *d*-wave resonance, referenced as "mixed" in Table 2. The fits with the lowest χ^2/NDF for the region below 1 MeV in resonance energy, for both the single and mixed cases, are the ones shown in Table 2. The rest of this paper relates to the findings in [43], including the comparisons with recent invariant mass measurements [38]; [40]; [42]; [29].

A comparison of the transfer measurement (for the case assuming a single state below 2 MeV) with some recent invariant mass measurement results is shown in Figure 1. Discrepancies clearly persist in the low-lying structure of ^{13}Be, even between recent measurements. The $\frac{5}{2}^+$ state is in a similar position in all the measurements; however, the width is much larger according to the works in [38] and [40]. Similarly, in [40] and [42], a broad $\frac{1}{2}^+$ structure below 1 MeV was shown, whereas [38] and [29] agree on an *s*-wave virtual state. There is some consistency in the presence of a *p*-wave resonance of approximately 0.5 MeV, with the exception of [40]. This resonance is noticeably narrower (Γ = 0.11 MeV) in the work in [43].

The mixed case in [43] is not shown in Figure 1 as the ordering of the *s*- and *p*-wave strength cannot be extracted from the data, only the relative intensities. The lowest χ^2/NDF was found for a mixture of $s - (70^{+8}_{-6}\%)$ and $p - (30^{+6}_{-8}\%)$ wave strengths. It should be noticed that the χ^2/NDF (3.87) for the $s - (93^{+2}_{-2}\%)$ and $d - (7^{+2}_{-2}\%)$ wave mixture below 1 MeV is similar to that for the *s*- and *p*-wave mixture (3.32). Therefore, the initial conclusion of the study was that the near-threshold strength was either a pure *p* wave or a mixture dominated by an *s*-wave strength, with a weaker resonance of either a *p*- or *d*-wave nature.

To make a more robust comparison between the recent invariant-mass measurements and the transfer reaction, the resonance parameters extracted from [38], [29], [40], and [42] were used as inputs for the Geant4 [47] simulation, as shown in Figure 2. The centroid energies and widths from the analyses were

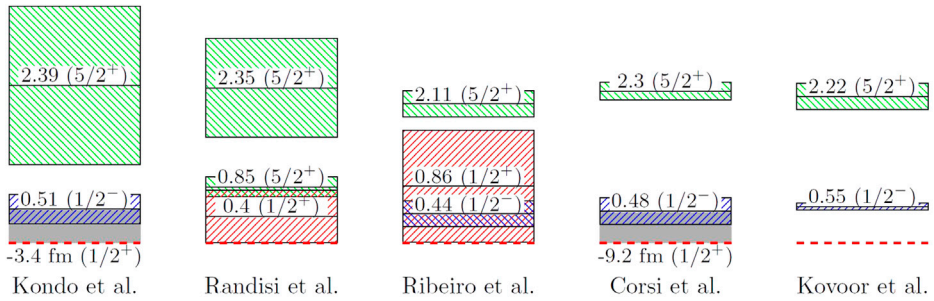

FIGURE 1
Comparison of the low-lying structure in ^{13}Be according to recent invariant mass measurements [38]; [40]; [42]; [29] and a recent transfer reaction measurement [43]. Only the case with a pure *p*-wave is shown for [43], as the position of the waves in the mixtures could not be resolved. Red, blue, and green lines depict *s*, *p*, and *d* waves, respectively. Red-dashed lines show the threshold. Gray-shaded region shows the presence of a virtual state.

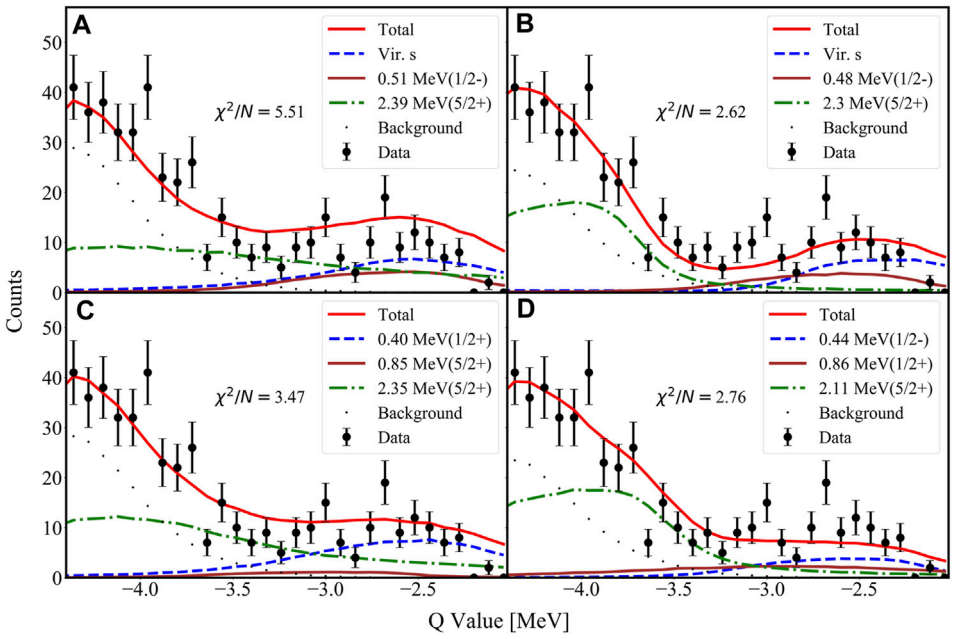

FIGURE 2
Data fitted with Geant4 simulations with energy and widths obtained from **(A)** [38], **(B)** [29], **(C)** [40], and **(D)** [42]. Amplitudes of the states were used from the angular distributions. Global fit is shown as the red line, and the background is denoted as black dots. Lowest-lying strength is shown as a blue-dashed line irrespective of its nature. Higher-lying states are depicted as solid brown and green dot–dashed lines.

used, and the relative intensities of the resonances and virtual states were fitted as free parameters. A relatively poor fit to the data from the ^{12}Be(d,p) reaction experiment was produced from the simulations using resonance parameters from [38] (χ^2/NDF = 5.51). Using the parameters from [40] provided a better fit (χ^2/NDF = 3.47), and those from [39] (not shown) provided a fit with χ^2/NDF = 3.18. The parameters that provided the best fit from the literature were those from [29] (χ^2/NDF = 2.62), closely followed by those from [42] (χ^2/NDF = 2.76). These can all be compared to the Bayesian fit of the data with a single *p*-wave resonance along with the well-known *d*-wave resonance of approximately 2 MeV. This fit allowed the locations and widths of the two resonances to vary along with the intensities. The parameters shown in Table 2 resulted in a χ^2/NDF of 2.02. The single *p* wave below the 2 MeV $\frac{5^+}{2}$ resonance is the scenario that best agrees with these data. This dominance of *p*-wave strength near the particle threshold is in agreement with the results of [27].

4 Summary

The beryllium chain of isotopes displays various clustering phenomena including molecular structures and one- and two-neutron halos in ^{11}Be and ^{14}Be, respectively. The isotope ^{13}Be is an unbound subsystem of the Borromean nucleus ^{14}Be. Its structure has been investigated experimentally for 40 years using both missing mass and invariant mass techniques. However, with the exception of the 2 MeV $\frac{5^+}{2}$ resonance, the low-lying structure is still disputed. A

new single-neutron transfer reaction experiment has brought new data and a new analysis technique involving Geant4 simulations and a Bayesian fitting routine. The best fit of the Q-value data was obtained with a narrow 0.55 MeV *p*-wave resonance and the *d*-wave resonance located at 2.22 MeV. Adding either a virtual state or a second resonance below 1 MeV produced somewhat poorer fits (χ^2/NDF = 3.0–3.4) that were dominated by the *s*-wave contribution (61%–89%) with a small *p*-wave (39%) or *d*-wave (11%) resonance. Using the resonance parameters from either [29] or [42] produced better fits to the new data from the literature. The literature resonance parameters producing poorer fits were those with a broader $\frac{5^+}{2}$ resonance [38]; [40].

Author contributions

KJ was the spokesperson for the new ^{12}Be + ^{2}H experiment and wrote the first draft of this manuscript. JK analyzed the data and produced the figures from the new ^{12}Be + ^{2}H experiment. RK was the co-spokesperson for the new ^{12}Be + ^{2}H experiment and was instrumental in the design and running of the experiment. All authors contributed to the article and approved the submitted version.

Funding

This research was supported by the U.S. Department of Energy, the Office of Science, the Office of Nuclear Physics under contract Nos DE-FG02-96ER40963 (UTK). The authors are grateful for the support from the NSERC, Canada Foundation for Innovation and Nova Scotia Research and Innovation Trust, and RCNP, the grant-in-aid program of the Japanese government. TRIUMF is supported by a contribution from the National Research Council, Canada.

Acknowledgments

The authors would like to acknowledge the collaborators on the TRIUMF ^{12}Be + ^{2}H experiment and the beam delivery team for providing the ^{12}Be beam, and DE-AC05-00OR22725 (ORNL), and the U. S. National Science Foundation under Award Numbers PHY-1404218 (Rutgers) and PHY-2011890 (Notre Dame). This work was supported by the National Research Foundation of Korea (NRF) grant funded by the Korean government (MSIT) grant nos 2020R1A2C1005981 and 2016R1A5A1013277. This work was partially supported by STFC grant no. ST/L005743/1 (Surrey).

Conflict of interest

The authors declare that the research was conducted in the absence of any commercial or financial relationships that could be construed as a potential conflict of interest.

Publisher's note

References

1. von Oertzen W. Two-center molecular states in ^{9}B, ^{9}Be, ^{10}Be, and ^{10}B. *Z Phys* (1996) 354:37–43. doi:10.1007/s002180050010

2. von Oertzen W. Dimers based on the $\alpha + \alpha$ potential and chain states of carbon isotopes. *Z Phys* (1997) 357:355–65. doi:10.1007/s002180050255

3. Seya M, Kohno M, Nagata S. Nuclear binding mechanism and structure of neutron-rich Be and B isotopes by molecular-orbital model. *Prog Th Phys* (1981) 65:204–23. doi:10.1143/PTP.65.204

4. Parfenova Y, Leclercq-Willain C. Hyperfine anomaly in be isotopes in the cluster model and the neutron spatial distribution. *Phys Rev C* (2005) 72:024312. doi:10.1103/PhysRevC.72.024312

5. Freer M, Horiuchi H, Kanada-En'yo Y, Lee D, Meißner U-G. Microscopic clustering in light nuclei. *Rev Mod Phys* (2018) 90:035004. doi:10.1103/RevModPhys.90.035004

6. Canavan R, Freer M. Demonstration of the universality of molecular structures in prolate deformed nuclei. *J Phys G* (2020) 47:095102. doi:10.1088/1361-6471/ab96b3

7. Nörtershäuser W, Tiedemann D, Žáková M, Andjelkovic Z, Blaum K, Bissell ML, et al. Nuclear charge radii of ^{7,9,10}Be and the one-neutron halo nucleus ^{11}Be. *Phys Rev Lett* (2009) 102:062503. doi:10.1103/PhysRevLett.102.062503

8. Krieger A, Blaum K, Bissell ML, Frömmgen N, Geppert C, Hammen M, et al. Nuclear charge radius of ^{12}Be. *Phys Rev Lett* (2012) 108:142501. doi:10.1103/PhysRevLett.108.142501

9. Fortier S, Pita S, Winfield J, Catford W, Orr N, de Wiele V, et al. Core excitation in ^{11}Be$_{gs}$ via the $p(^{11}Be,^{10}Be)d$ reaction. *Phys Lett* (1999) B461:22–7. doi:10.1016/S0370-2693(99)00825-4

10. Deltuva A, Ross A, Norvaišas E, Nunes FM. Role of core excitation in (*d, p*) transfer reactions. *Phys Rev C* (2016) 94:044613. doi:10.1103/PhysRevC.94.044613

11. Moro AM, Crespo R. Core excitation effects in the breakup of the one-neutron halo nucleus ^{11}be on a proton target. *Phys Rev C* (2012) 85:054613. doi:10.1103/PhysRevC.85.054613

12. Nunes FM, Thompson IJ, Tostevin JA. Core excitation in ^{12}Be. *Nucl Phys* (2002) A703:593–602. doi:10.1016/S0375-9474(01)01667-0

13. Nunes FM. Valence pairing, core deformation and the development of two-neutron halos. *Nucl Phys* (2005) A757:349–59. doi:10.1016/j.nuclphysa.2005.04.005

14. Descouvemont P. Halo structure of ^{14}Be in a microscopic ^{12}Be+n+n cluster model. *Phys Rev C* (1995) 52:704–10. doi:10.1103/PhysRevC.52.704

15. Thompson IJ, Zhukov MV. Structure and reactions of the ^{12,14}Be nuclei. *Phys Rev C* (1996) 53:708–14. doi:10.1103/PhysRevC.53.708

16. Labiche M, Marqués FM, Sorlin O, Vinh Mau N. Structure of ^{13}Be and ^{14}Be. *Phys Rev C* (1999) 60:027303. doi:10.1103/PhysRevC.60.027303

17. Vinh Mau N, Pacheco JC. Structure of the ^{11}Li nucleus. *Nucl Phys* (1996) A607:163–77. doi:10.1016/0375-9474(96)00246-1

18. Spyrou A, Smith JK, Baumann T, Brown BA, Brown J, Christian G, et al. Search for the ^{15}be ground state. *Phys Rev C* (2011) 84:044309. doi:10.1103/PhysRevC.84.044309

19. Spyrou A, Kohley Z, Baumann T, Bazin D, Brown BA, Christian G, et al. First observation of ground state dineutron decay: ^{16}Be. *Phys Rev Lett* (2012) 108:102501. doi:10.1103/PhysRevLett.108.102501

20. Poppelier N, Wood L, Glaudemans P. Properties of exotic p-shell nuclei. Phys Lett *B* (1985) 157:120–2. doi:10.1016/0370-2693(85)91529-1

21. Fortune HT. Update on energies and widths in ^{13}Be. *Phys Rev C* (2019) 99:014304. doi:10.1103/PhysRevC.99.014304

22. Macchiavelli AO, Crawford HL, Campbell CM, Clark RM, Cromaz M, Fallon P, et al. Analysis of spectroscopic factors in ^{11}Be and ^{12}Be in the Nilsson strong-coupling limit. *Phys Rev C* (2018) 97:011302. doi:10.1103/PhysRevC.97.011302

23. Descouvemont P. Evidence for particle stability of ^{13}Be in a microscopic cluster model. Phys Lett *B* (1994) 331:271–5. doi:10.1016/0370-2693(94)91050-2

24. Kanada-En'yo Y. Breaking of N=8 magicity in ^{13}Be. *Phys Rev C* (2012) 85:044320. doi:10.1103/PhysRevC.85.044320

25. Ren Z, Chen B, Ma Z, Xu G. Level inversion of N=9 isotones in the relativistic mean-field theory. *Z Phys A* (1997) 357:137–41. doi:10.1007/s002180050228

26. Bonaccorso A. Unbound nuclei studied by projectile fragmentation. *Physica Scripta* (2012) 2012:014008. doi:10.1088/0031-8949/2012/t150/014008

27. Casal J, Gómez-Ramos M, Moro A, Corsi A. Exploring continuum structures in reactions with three-body nuclei. *J Phys Conf Ser* (2020) 1643, 012075. doi:10.1088/1742-6596/1643/1/012075

28. Thompson I, Nunes F, Danilin B. FaCE: A tool for three body faddeev calculations with core excitation. *Comp Phys Commun* (2004) 161:87–107. doi:10.1016/j.cpc.2004.03.007

29. Corsi A, Kubota Y, Casal J, Gómez-Ramos M, Moro A, Authelet G, et al. Structure of ^{13}Be probed via quasi-free scattering. *Phys Lett B* (2019) 797:134843. doi:10.1016/j.physletb.2019.134843

30. Ostrowski AN, Bohlen HG, Demyanova AS, Gebauer B, Kalpakchieva R, Langner C, et al. Mass spectroscopy of ^{13}Be. *Z Phys* (1992) A343:489–90. doi:10.1007/BF01289828

31. Aleksandrov DV, Ganza EA, Glukhov YA. Observation of the isotope ^{13}Be in the reaction ^{14}C(^{7}Li, ^{8}B). *Sov J Nucl Phys* (1983) 37:474–5.

32. von Oertzen W, Bohlen H, Gebauer B, von Lucke-Petsch M, Ostrowski A, Seyfert C, et al. Nuclear structure studies of very neutron-rich isotopes of $^{7-10}$He, $^{9-11}$Li and $^{12-14}$Be via two-body reactions. *Nucl Phys A* (1995) 588:c129–34. Proceedings of the Fifth International Symposium on Physics of Unstable Nuclei. doi:10.1016/0375-9474(95)00111-D

33. Belozyorov A, Kalpakchieva R, Penionzhkevich Y, Dlouhý Z, Piskor S, Vincour J, et al. Spectroscopy of ^{13}Be. *Nucl Phys A* (1998) 636:419–26. doi:10.1016/S0375-9474(98)00217-6

34. Korsheninnikov A, Nikolskii E, Kobayashi T, Aleksandrov D, Fujimaki M, Kumagai H, et al. Spectroscopy of ^{12}Be and ^{13}Be using a ^{12}Be radioactive beam. *Phys Lett B* (1995) 343:53–8. doi:10.1016/0370-2693(94)01435-F

35. Thoennessen M, Yokoyama S, Hansen PG. First evidence for low lying s-wave strength in ^{13}Be. *Phys Rev C* (2000) 63:014308. doi:10.1103/PhysRevC.63.014308

36. Lecouey JL. Experimental studies of unbound neutron-rich nuclei. *Few-Body Syst* (2004) 34:21–6. doi:10.1007/s00601-004-0029-3

37. Simon H, Meister M, Aumann T, Borge M, Chulkov L, Pramanik UD, et al. Systematic investigation of the drip-line nuclei ^{11}Li and ^{14}Be and their unbound subsystems ^{10}Li and ^{13}Be. *Nucl Phys A* (2007) 791:267–302. doi:10.1016/j.nuclphysa.2007.04.021

38. Kondo Y, Nakamura T, Satou Y, Matsumoto T, Aoi N, Endo N, et al. Low-lying intruder state of the unbound nucleus ^{13}Be. *Phys Lett B* (2010) 690:245–9. doi:10.1016/j.physletb.2010.05.031

39. Aksyutina Y, Aumann T, Boretzky K, Borge MJG, Caesar C, Chatillon A, et al. Structure of the unbound nucleus ^{13}Be: One-neutron knockout reaction data from ^{14}Be analyzed in a holistic approach. *Phys Rev C* (2013) 87:064316. doi:10.1103/PhysRevC.87.064316

40. Randisi G, Leprince A, Al Falou H, Orr NA, Marqués FM, Achouri NL, et al. Structure of ^{13}Be probed via secondary-beam reactions. *Phys Rev C* (2014) 89:034320. doi:10.1103/PhysRevC.89.034320

41. Marks BR, DeYoung PA, Smith JK, Baumann T, Brown J, Frank N, et al. Population of ^{13}Be in a nucleon exchange reaction. *Phys Rev C* (2015) 92:054320. doi:10.1103/PhysRevC.92.054320

42. Ribeiro G, Nácher E, Tengblad O, Díaz Fernández P, Aksyutina Y, Alvarez-Pol H, et al. Structure of ^{13}Be studied in proton knockout from ^{14}B. *Phys Rev C* (2018) 98:024603. doi:10.1103/PhysRevC.98.024603

43. Kovoor J, et al. Structure studies of ^{13}Be accepted. *Phys Rev C* (2023).

44. Kovoor JM. *Study of one-nucleon transfer reactions*. Phd dissertation. Knoxville: University of Tennessee (2022).

45. Kanungo R. Iris: The ISAC charged particle reaction spectroscopy facility for reaccelerated high-energy ISOL beams. *Hyperfine Interactions* (2014) 225:235–40. doi:10.1007/s10751-013-0904-8

46. Hooker J, Kovoor J, Jones K, Kanungo R, Alcorta M, Allen J, et al. Use of Bayesian Optimization to understand the structure of nuclei. *Nucl Instrum Methods B* (2022) 512:6–11. doi:10.1016/j.nimb.2021.11.014

47. Agostinelli S, Allison J, Amako K, Apostolakis J, Araujo H, Arce P, et al. Geant4-a simulation toolkit. *Nucl Instrum Methods A* (2003) 506:250–303. doi:10.1016/S0168-9002(03)01368-8